Rapid responses of the cupula in the lateral line of ruffe (Gymnocephalus cernuus)

Curcic-Blake, B; van Netten, SM

Published in:
Journal of comparative physiology a-Neuroethology sensory neural and behavioral physiology

DOI:
10.1007/s00359-005-0599-7

Publication date:
2005

J Comp Physiol A (2005) 191: 393–401
DOI 10.1007/s00359-005-0599-7

ORIGINAL PAPER

Branislava Ćurčić-Blake · Sietse M. van Netten

Rapid responses of the cupula in the lateral line of ruffe (*Gymnocephalus cernuus*)

Received: 23 August 2004 / Revised: 6 December 2004 / Accepted: 8 December 2004 / Published online: 18 February 2005

Abstract Displacements of cupulae in the supraorbital lateral line canal in ruffe (*Gymnocephalus cernuus*) have been measured using laser interferometry and by applying transient as well as sinusoidal fluid stimuli in the lateral line canal. The cupular displacement in response to impulses of fluid velocity shows damped oscillations at approximately 120 Hz and a relaxation time-constant of 4.4 ms, commensurate with a quality factor of approximately 1.8. These values are in close agreement with the frequency characteristics determined via sinusoidal fluid stimuli, implying that the nonlinearity of cupular dynamics imposed by the gating apparatus of the sensory hair cells is limited in the range of cupular displacements and velocities measured (100–300 nm; 100–300 μm/s). The measurements also show that cupular displacement instantaneously follows the initial waveform of transient stimuli. The functional significance of the observed cupular dynamics is discussed.

Keywords Lateral line · Cupula · Mechanical impulse response · Hair cells · Laser interferometry

Abbreviations FFT: Fast Fourier transform · ILPM: Incident light polarizing microscopy

Introduction

The mechano-sensory lateral line organ of fish and aquatic amphibians, like the inner ear and vestibular system, belongs to the acoustico-lateralis system. The lateral line organ is used by aquatic animals to detect water vibrations relative to their bodies at frequencies below a few hundred Hertz (Dijkgraaf 1963; Coombs and Janssen 1990; Bleckmann 1993). The mechano-sensory lateral line organ is used for prey detection (Hoekstra and Janssen 1985; Montgomery and Macdonald 1987; Enger et al. 1989), intraspecific communication (Partridge and Pitcher 1980; Satou et al. 1994), stationary object detection (Dijkgraaf 1963; Abdel-Latif et al. 1990) and rheotaxis (Montgomery et al. 1997).

Neuromasts are the functional peripheral detection units of the lateral line organ. These detection units consist of groups of mechano-sensory hair cells covered with an aqueous cupula and may be situated on the skin (superficial neuromasts) or in a system of sub-epidermal canals (canal neuromasts), which are only present in fish. In both subsystems the lateral line organ is distributed along the body or, in fish, runs laterally along the trunk. Neuromasts are mechanically stimulated via their cupulae. Cupulae are hydrodynamically excited by the fluid that flows past them, which is either the canal lymph (canal neuromasts), or the surrounding water (superficial neuromasts). Cupulae slide along the sensory epithelium so that the bundles of hair cells, protruding into the cupular base, are deflected. Deflection of the bundles causes hair cell transducer channels to open (Hudspeth et al. 2000), which starts a cascade of events leading eventually to hair cell depolarisation that triggers action potentials in afferent nerves (e.g. Russel 1976; Kroese and van Netten 1989). This stimulus-coded afferent activity is transferred to the central nervous system for further processing.

The dynamics of the cupula of the ruffe (*Gymnocephalus cernuus*) in the supra-orbital canal has been investigated previously using experimental techniques to determine its mechanical responses to sinusoidal fluid displacement produced in the canal in the frequency range of a few Hertz up to several hundreds of Hertz (van Netten and Kroese 1987). In combination with theoretical calculations, the measured frequency characteristics could be explained in terms of a frequency-dependent

B. Ćurčić-Blake · S. M. Netten (✉)
Department of Neurobiophysics,
University of Groningen, Nijenborgh 4,
9747 Groningen, The Netherlands
E-mail: b.curcic@phys.rug.nl
E-mail: s.van.netten@phys.rug.nl
Tel.: +31-50-3634741
Fax: +31-50-3634740

boundary layer driving the cupula (van Netten 1991). At frequencies ranging from DC to between 10 Hz and 20 Hz, cupulae are displaced in proportion to fluid velocity, and thus can be considered pure detectors of fluid velocity (Denton and Gray 1983; Kalmijn 1988). Beyond these frequencies the cupula acts as a detector of a frequency-dependent combination of fluid velocity and acceleration up to the resonance frequency, which occurs on average at approximately 120 Hz and is related to hair bundle stiffness in combination with cupular and fluid mass. At frequencies beyond that of the resonance the cupula tends to move in phase and with the same amplitude as the excitatory fluid, because stiffness forces become negligible compared to inertial forces.

Remarkably, the rather complex cupular mechanics, together with the filtering of viscous fluid flow controlled by the canal (Denton and Gray 1983), leads to a nearly flat cupular frequency response below the resonance frequency, when referred to the acceleration of outside-water flow relative to the fish body. The overall peripheral acceleration sensitivity, which was experimentally observed in afferent neural activity of ruffe (Wubbels 1992) as well as in several canal systems of other fish species (Coombs and Janssen 1990; Kroese and Schellart 1992; Engelmann et al. 2000), can be explained by the compensatory effects of canal and cupular hydrodynamics (S.M. van Netten (submitted)).

Under natural conditions, various events present hydrodynamic stimuli to the neuromasts of the lateral line organ. There are only a few reports, however, on the physical characteristics of the water motion under these conditions, such as that produced by other aquatic animals (Kalmijn 1989; Enger et al. 1989; Bleckmann et al. 1991). The frequency content of hydrodynamic signals produced by hovering or approaching fish or by obstacles in running water, represented in terms of water acceleration, was found to be most significant at frequencies lower than approximately 100 Hz. This range corresponds well to the range of frequencies at which the canal lateral line organ has a constant acceleration sensitivity and has been put forward as support for considering the canal lateral line system to be a low frequency water acceleration detection apparatus (Kalmijn 1988).

The mechanical responses of the cupula to stimuli that simulate transient characteristics occurring in natural conditions have not been investigated in detail so far. As a first step, we present here cupular displacement data on responses to fast transient stimuli in the form of water motion produced in the canal. Such responses need not necessarily be the same as the inverse Fourier transform of the previously measured and modelled cupular frequency characteristics, since cupular mechanics has been shown to be nonlinear (van Netten and Khanna 1994). It has been demonstrated that the hair cell gating apparatus imposes its effective nonlinear stiffness on cupular mechanics via the bundles of the hair cell. In addition, other active hair bundle mechanics such as nonlinear adaptation (Eatock 2000) may influence the detailed responses in the time domain.

In order to investigate the time characteristics of the peripheral lateral line organ with respect to transient stimuli, we have measured cupular responses to a filtered fluid step stimulus. This approach provides direct information on the timing and speed of the lateral system under in vivo conditions.

Materials and methods

Preparation

Experiments were performed on the supraorbital lateral line of ruffe (*Gymnocephalus cernuus*) ($n = 9$) with body lengths ranging from 10–12.5 cm. Fish were anaesthetised with an intraperitoneal injection (60 mg/kg of body weight) of Saffan (Mallinckrodt Veterinary, Uxbridge, UK) and subsequently placed in a fish tank-holder, held firmly by head and body clamps while they were respired by a flow of tap water through their gills. The skin and the bony bridge covering the supraorbital canal neuromast no. 3 (Jakubowski 1963) were carefully removed. Cupulae were optically monitored by an incident light polarising microscope (ILPM; Kroese and van Netten 1987) via a small mirror placed beneath the cupulae in the orbit. The condition of the fish was determined by inspecting the blood flow through capillaries in the eye, and the condition of the neuromast was determined by inspection of the blood flow through capillary vessels in the macula.

Mechanical stimulation

Cupulae were stimulated with a sphere producing either a step (Stimulus I) or a sinusoidal (Stimulus II) displacement (amplitude range 100–300 nm) of the local fluid flow past the cupula. In seven experiments a sphere with a diameter of 6.4 mm was used and was placed in front of the cupula just outside the canal (width ~1 mm). A smaller stimulus sphere (Ø~0.8 mm) used in two experiments allowed placement in the canal at a distance of approximately 4 mm in front of the cupula. In both cases the spheres were attached to a piezo-electric driver, generating a movement of the sphere parallel to the longitudinal axis of the canal, the direction in which the hair cells underneath the cupula are most sensitive. No significant differences in cupular frequency characteristics were found using the two stimulus spheres.

Step displacements (Stimulus I) of the sphere were used in order to obtain impulse responses of the cupula. A step displacement of a sphere produces a step displacement of the water in the canal (e.g. Fig. 9 in Tsang 1997; Tsang and van Netten 1997). The velocity of both the sphere and water to which the cupula responds is therefore a pulse. Its duration is determined by a low-pass filter (cut-off frequency 850 Hz, 8-pole Bessel, Krohn-Hite, 3988), that shapes the input signal to the piezo-electric driver, preventing the sphere and its

support rod from mechanically oscillating at its resonance of approximately 1 kHz. The stimulus sphere and the generated fluid displacement step have a finite (1.2 ms) rise-time as a consequence (e.g. Figs. 1 and 2). A typical cupula has its resonance in the range 100–200 Hz and is therefore negligibly affected by the filter in its physiologically relevant frequency range. The protocol for the step displacement (Stimulus I) of a sphere is presented in Fig. 1. The positive voltage step occurs at $t = 0$ ms and the negative step starts at $t = 130$ ms.

Series of sinusoidal displacements (Stimulus II) of the sphere with frequencies in the range of 10–500 Hz were used to obtain direct frequency response curves of the cupula.

Displacement measurement of cupula and sphere

Cupular motion was measured using a differential laser interferometer coupled to an incident light polarizing microscope (ILPM; Kroese and van Netten 1987; van Netten and Kroese 1987). In short, two laser beams were focused on a location inside the transparent cupula, where a scattering optical irregularity causes interference. The backscattered light, detected with a photomultiplier (Hamamatsu, R1477), was phase shifted in proportion to the displacement of the cupula, and therefore uniquely coded the information on the motion of the cupula.

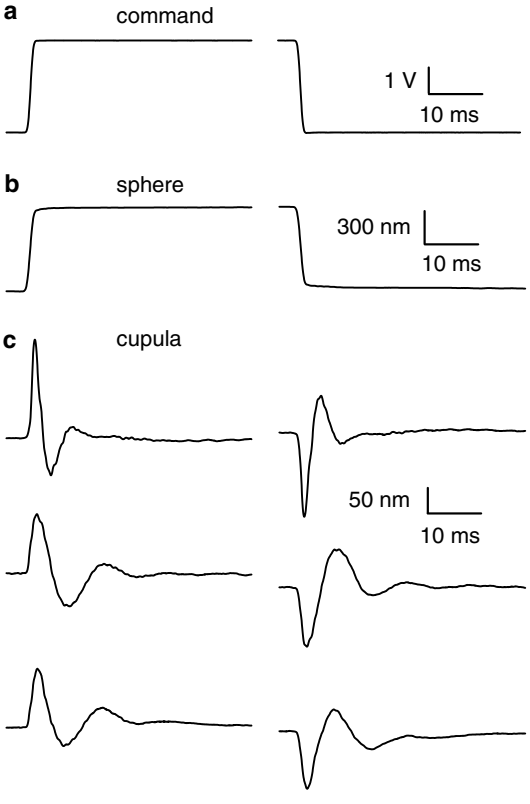

Fig. 1 Step protocol (Stimulus I) and induced cupular responses. The command voltage (**a**) is either a step-up or step-down. The stimulus sphere (**b**) follows the command voltage applied to the piezo-driver. Responses of three different cupulae are presented in the three lower traces (**c**)

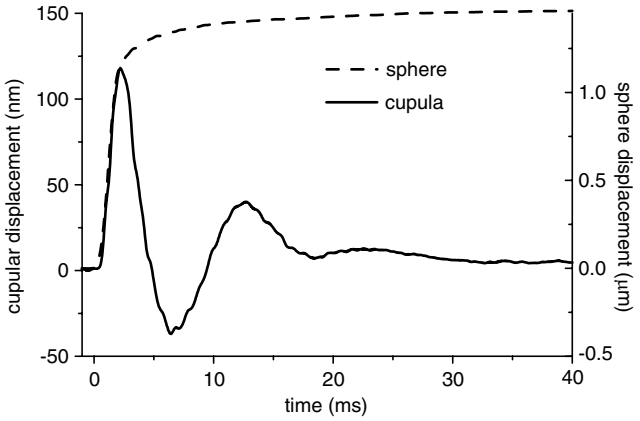

Fig. 2 The impulse response of the cupula follows the initial displacement of the sphere with a time delay less than the measurement accuracy (< 0.1 ms)

The photomultiplier output was processed with a modified demodulator (Polytec, OVF 3000), which has two calibrated output modes representing velocity (analog decoder) and displacement (digital decoder). Displacement, after averaging (50–500×), was determined with an accuracy ranging from 1.5 nm to 4.5 nm (r.m.s. noise equivalent displacement). In the experiments using the 1 mm diameter stimulus sphere, velocity was measured simultaneously with displacement, with an accuracy of 0.6 µm/s (r.m.s. noise equivalent velocity). Displacement and velocity signals were low-pass filtered using an 8-pole Bessel filter and amplified (Stimulus I: Krohn-Hite, $f_{co} = 850$ Hz; Stimulus II: Frequency Devices, f_{co} set at eight times the stimulus frequency). Measured signals were digitised with a 16-bit A/D converter (Ariel, DSP-16). The sampling frequency was 16 kHz in the case of the step stimuli (Stimulus I), and 32 times the stimulus frequency in the case of the sinusoidal stimulus (Stimulus II).

Frequency responses (based on both Stimulus I and II) were corrected for the frequency characteristics of the stimulus sphere system, amplifiers and filters.

Cupular frequency characteristics from impulse responses

Displacements of the cupula in response to a step sphere displacement (stimulus I) were measured as a function of time. Cupular displacement responses are proportional to fluid velocity over a considerable (low) frequency range, and the cupula can therefore be considered as a detector of fluid velocity in this range (Kalmijn 1988, 1989; Kroese et al. 1978). Since a fluid displacement step is equivalent to a fluid velocity impulse, we will define the displacement of the cupula in response to a fluid displacement step as a cupular impulse response. Frequency characteristics of the cupula based on stimulus

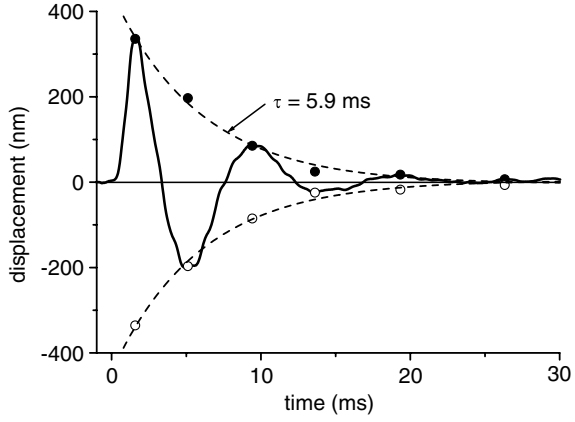

Fig. 3 Determination of the relaxation time τ of the cupula. The *solid line* shows a measured impulse response. *Circles* indicate the extremes of the measured impulse response. The *dashed lines* represent the fitted single exponential function from which τ was obtained

protocol I were determined by taking the fast Fourier transform (FFT) of the impulse response. The results are presented as the displacement of the cupula as a function of frequency of either (constant amplitude) water displacement (Fig. 4a; e.g. van Netten 1991) or water velocity (Fig. 4b; e.g. S.M. van Netten (submitted)).

Determination of Q factor, resonance frequency and relaxation time constant

Stimulus I

Impulse responses measured using stimulus I are damped oscillations (see Fig. 1), from which the quality factor Q_I was determined as:

$$Q_I = \frac{\pi}{\ln\left(A_1/A_3\right)} \quad (1)$$

where A_1 and A_3 are the first and third extreme displacements of the cupula from the equilibrium position. The resonance frequency of the cupula for stimulus I (f_{rI}) was calculated from the period of the damped oscillations using:

$$f_{rI} = \frac{1}{\Delta t_{zc}}, \quad (2)$$

where Δt_{zc} is the time between the onset of the stimulus and the moment at which the cupula crosses its equilibrium position for the second time after the onset (see Fig. 2).

The relaxation time constant, τ, of the cupula was determined from measured impulse responses that were rectified so that displacement maxima could be resolved. This usually resulted in between 5 and 7 points defining the envelope of the oscillations, to which a single exponential function was fitted. The time constant of the exponential function was taken as the relaxation time constant of the cupula, τ (see Fig. 3).

Stimulus II

Using stimulus II (sinusoidal fluid flow), both measures of the frequency characteristics, Q and f_r, were determined from fits to directly measured frequency responses using a previously described cupular dynamics model (van Netten 1991). This mathematical model was derived under the assumption that the viscous fluid in the canal is Newtonian, incompressible, spatially uniform and linear and that the cupula is elastically coupled with stiffness S to the underlying sensory epithelium.

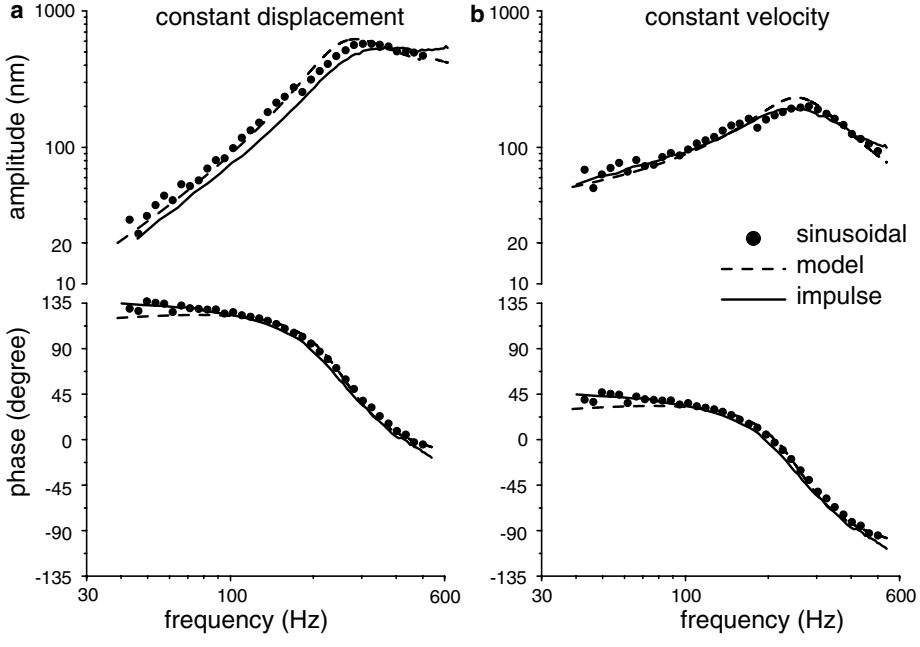

Fig. 4 Frequency responses of the cupula. **a** Cupular displacement (*upper panel*) and phase (*lower panel*) versus frequency of a constant fluid displacement amplitude. Data points represent measured cupular displacement in response to a series of frequencies. The *dashed lines* show a model fit ($N_r = 49$; $f_t = 30$), while the *solid lines* depict the frequency response calculated from measured impulse responses. **b** Same as in (**a**) but amplitude and phase are shown as a function of frequency of constant amplitude fluid velocity

Stokes' analysis (Stokes 1851) was used to calculate the fluid forces acting on the cupula. The complex displacement amplitude, X_0, of a cupula with radius a, in response to fluid with density ρ, viscosity μ and a velocity amplitude V_0 at frequency f, is then (e.g. S.M. van Netten (submitted)):

$$X_0 = V_0 \frac{1}{2\pi f_t} \frac{1 + \frac{1}{2}\sqrt{2}(i+1)(f/f_t)^{1/2} + \frac{i}{3}(f/f_t)}{N_r + i(f/f_t) - \frac{1}{2}\sqrt{2}(1-i)(f/f_t)^{3/2} - \frac{1}{3}(f/f_t)^2} \tag{3a}$$

$$N_r = \frac{Sa\rho}{6\pi\mu^2} \quad f_t = \frac{\mu}{2\pi\rho a^2} \tag{3b}$$

Here, the dimensionless resonance number, N_r, determines the extent of resonance, whereas the transition frequency, f_t, indicates the frequency at which inertial fluid forces start to dominate the viscous fluid forces acting on the cupula.

Fitting of the model to obtain the parameters N_r and f_t was done by eye. The quality factor Q_{II} was subsequently determined using (van Netten 1991):

$$Q_{II} = \sqrt{\frac{2}{3}}\left(\frac{N_r}{3}\right)^{1/4} \tag{4}$$

The resonance frequency of the cupula, f_{rII}, was determined by the maximum of the model curve fitted to the data.

Results

Cupular displacements and velocities were measured in response to hydrodynamic stimulation using two types of stimulus protocols. The first type consisted of fluid displacement step stimuli, equivalent to fluid velocity pulses (Stimulus I), whereas the second type consisted of successive series of sinusoidal fluid flows at different frequencies to determine directly the cupular frequency responses (Stimulus II). Responses to stimulus protocol I were analysed as described in the methods section and were subsequently compared to those obtained using stimulus protocol II.

Cupular impulse responses

Stimulus protocol I together with induced displacements of stimulus sphere and cupulae are shown in Fig. 1. The step of the command voltage to the piezo-driver and the measured displacement of the stimulating sphere, which is attached to the driver, are displayed in the two top traces (Fig. 1a, b). The rise time of the sphere is approximately 1.2 ms and is restricted by filtering the command voltage signal to avoid strong mechanical resonance behaviour of the piezo-electrically driven stimulus sphere. Displacement steps of the stimulus sphere were in the range of 1–3 μm and its related impulse velocities were in the range of approximately 1–3 mm/s. Displacement traces (Fig. 1c) are depicted for three different cupulae of three different fish. The positive direction of displacement is defined as being directed from the head towards the tail of the fish. Positive displacements of the sphere induce initial positive displacements of the cupulae. For displacement steps of the sphere in the negative direction the initial cupular responses are accordingly reversed, as indicated in the second half of the time responses of the cupulae (Fig. 1). The cupular responses follow the initial motion of the stimulus sphere and subsequently show oscillations around the equilibrium position, reminiscent of the resonance behaviour of the cupula. The related initial cupular velocity is approximately 125 μm/s. The typical range of initial cupular velocities was 100–300 μm/s. A more detailed comparison of the cupular response with the stimulus sphere displacement is shown in Fig. 2. It appears that up to approximately the first maximum the cupula follows the displacement step of the sphere without significant time delay.

The cupular displacement responses to the fluid displacement steps clearly resemble that of a damped oscillator. After tens of milliseconds the envelope of the oscillations declines to zero. As is obvious from Fig. 1, the induced cupular oscillations differ in amplitude and time duration among different cupulae. Oscillatory details in the measured step responses that describe the variations among different fish and that enable the analysis of the frequency characteristics in terms of the quality factor (Q_I) and resonance frequency (f_{rI}) are the timing (t_i) and amplitude (A_i) of the first three extremes of cupular displacement from the equilibrium position (Fig. 1). The amplitude of the first maximum is a measure of the fluid displacement in the immediate neighbourhood of the cupula and therefore probably does not reflect specific cupular properties (see also Discussion). The second extreme of the displacement occurs at t_2, which is 4.1 ± 1.7 ms ($n = 9$) after the first extreme, in the opposite direction, with an amplitude A_2 which amounts to $40.5 \pm 16.8\%$ ($n = 9$) of A_1. The third extreme of the displacement occurs at t_3, which is 8.4 ± 2.7 ms after the first, in the fluid step direction, with an amplitude A_3, equal to $16.7 \pm 8.2\%$ of A_1.

Relaxation time-constants, τ, were determined by fitting a single exponential function to the envelope of the damped oscillations defined by the extreme displacements (see Fig. 3), yielding $\tau = 4.4 \pm 2.7$ ms ($n = 9$).

Comparison of cupular frequency characteristics

The frequency characteristics of impulse responses (Stimulus I) were calculated and then compared with the frequency characteristics directly measured in response to a series of sinusoidal stimuli (Stimulus II). Comparisons of the two types of frequency characteristics are presented in Fig. 4, which shows the cupular

displacement as a function of frequency of excitatory fluid flow with constant displacement amplitude (Fig. 4a). Since lateral line cupulae can be considered to be detectors of fluid velocity in a restricted low-frequency range (Denton and Gray 1983; Kalmijn 1989; e.g. S.M. van Netten (submitted)), the data of Fig. 4a have been replotted in Fig. 4b as a function of frequency of excitatory fluid flow with a constant velocity amplitude (as described in Eq. 3a, b). The associated phase difference of 90° is due to the phase difference between displacement and velocity. Figure 4b indicates that at approximately 250 Hz the displacement of the supraorbital canal neuromast in ruffe is enhanced by at least a factor of 4 with respect to that at low frequencies (~ 40 Hz), due to resonance. This observation supports the notion that this type of canal cupula cannot be considered a pure detector of velocity (e.g. van Netten 1991, (submitted)).

In general, a comparison of the frequency characteristics obtained from FFT's of the impulse responses (Stimulus I, solid lines, Fig. 4) with the directly measured frequency responses (Stimulus II, data points, Fig. 4) shows many similarities. Model fits to the data are shown by the dashed lines in Fig. 4. Most of the cupulae follow the model description of Eq. 2 well into the region of their best frequency. Using the model, the resonance number N_r was found to be 69 ± 52 ($n = 7$) and the transition frequency f_t was 16 ± 10 Hz ($n = 7$).

From the damped cupular oscillations (Stimulus I), the quality factor of the cupula, Q_I, was determined directly from the measurements, using Eq. 1, and was found to be 1.8 ± 0.5 ($n = 9$). The quality factor obtained from the N_r number in combination with Eq. 4 was $Q_{II} = 1.7 \pm 0.3$ ($n = 7$), which is in good agreement with Q_I.

The inverse of the period of the first full oscillation cycle of an impulse response was used to directly determine the resonance frequency of the cupula. The resulting resonance frequency is $f_{rI} = 121 \pm 56$ Hz ($n = 7$, Stimulus I; Eq. 2), which is comparable to that found from measured frequency responses of the same cupulae. Use of the model description yielded the resonance frequency $f_{rII} = 128 \pm 60$ Hz ($n = 7$, Stimulus II). It is evident from Fig. 1 that the duration of the first period, and therefore the best frequency, varies among different cupulae as indicated by the significant standard deviations (SD). A linear regression procedure on the resonance frequencies, f_{rI} and f_{rII}, obtained using the two stimulus protocols, yielded a correlation coefficient of 0.99 ($P < 0.0003$), thus confirming that the two stimulus methods produce similar results and that the SD of their means arise from individual neuromast differences.

Results for the various measurements of the frequency characteristics and model results for individual cupulae are summarised in Table 1.

Discussion

Damped cupular impulse responses are consistent with frequency responses

The displacement of the cupula in the supraorbital lateral line canal of ruffe was measured in response to velocity pulses (impulses, Stimulus I). Figure 1 presents typical examples of such impulse responses of three cupulae in three different fish, which exhibit damped resonance behaviour around their equilibrium position at frequencies of $f_{rI} = 121 \pm 56$ Hz and with a quality factor of $Q_I = 1.8 \pm 0.5$. These variations in frequency characteristics are thought to be due to variations in the physical parameters of the peripheral lateral line system, such as the dimensions of the cupula and its elastic coupling to the canal (Wiersinga-Post and van Netten 2000). This is supported by the high correlation of the two resonance frequencies obtained using the two stimulus methods for individual cupulae. Indeed, similar values of the resonance frequency, $f_{rII} = 128 \pm 60$ Hz, and quality factor, $Q_{II} = 1.7 \pm 0.3$, were obtained from the measured frequency characteristics using sinusoidal water motion (Stimulus II) in combination with fitting a cupular dynamics model to the measured data. The two independent parameters of the model (Eq. 3a, b) are the resonance number ($N_r = 69$) and the transition frequency ($f_t = 16$ Hz). The values found are in line with previous results on cupular dynamics of the ruffe (Wiersinga-Post and van Netten 2000). Moreover, taking the FFT of the

Table 1 Summary of results of cupular parameters

	Q_I	Q_{II}	f_{rI} (Hz)	f_{rII} (Hz)	f_t (Hz)	N_r	τ (ms)
3815	1.7	1.6	238	256	30	49	1.8
3806	1.5	1.2	121	121	30	16	2.7
3728	1.3		113				2.3
3725	1.2						2.4
3723	1.7	1.8	86	85	8	70	7.7
3721	2.7	1.6	76	98	12	44	1.8
3718	1.5	1.6		128	16	42	8.7
3714	2.2	2.3	84	84	5	174	6.0
3711	2.3	1.9	131	126	10	90	5.9
Mean ± SD	1.8 ± 0.5	1.7 ± 0.3	121 ± 56	128 ± 60	16 ± 10	69 ± 52	4.4 ± 2.7

Subscripts I and II denote parameters obtained by using Stimulus I and Stimulus II, respectively. The table lists values of quality factors (Q_I and Q_{II}), resonant frequencies (f_{rI} and f_{rII}), values of resonance number (N_r) and transition frequency (f_t) and relaxation time constant (τ). Mean values are given with standard deviations. The first column refers to the code used for individual experiments

measured impulse responses allowed a more detailed comparison of the two types of responses to be made and confirmed their general similarity, although small differences are also visible. The low-frequency region is difficult to measure since the cupula shows a decreased response at lower frequencies, which may become smaller than the measurement threshold.

An important implication of the above similarity of the results obtained using the two stimulus protocols is that the peripheral mechanics of the lateral line system behaves essentially linearly in response to the two types of stimuli presented. Nonlinearity of cupular mechanics, imposed by the gating compliance of the transducer channels of the hair bundle (van Netten and Khanna 1994), therefore does not significantly seem to affect the timing of transient cupular dynamics in response to velocity pulses. Nonlinearity of lateral line cupular mechanics was observed in a different fish species (*Xenomystus nigri*). It is not likely, however, that the gating compliance is significantly different across species. The displacement-dependent gating compliance, under the conditions of the presently measured impulse responses, are probably most apparent during the initial phase of cupular impulse response. During this phase, bundle deflections are predominantly in the range of 100 nm and beyond, so that the cupular sliding stiffness may be reduced due to the gating compliance of the hair bundles. During the decaying phase, about 10 ms after onset of the impulse response, the cupula spends relatively more time in the linear stiffness range.

To test for this manifestation of nonlinear gating compliance in cupular impulse responses, we attempted to take an opposite approach: calculating the impulse responses of a cupula by taking the inverse FFT of a frequency response of the fitted linear model (Eq. 3a, b). Comparisons of the measured and simulated impulse responses, including the filters as used in the experiments, are shown in Fig. 5. Again, the general shape of both responses is similar, but differences can also be discerned. Most significantly, it proved to be impossible to simulate the details in the crossings of the cupular equilibrium position. When the model parameters were adjusted so as to obtain a resonance frequency equal to the best frequency of the impulse response f_{rI}, accomplished by taking equal periods of the first oscillation cycle of modelled and measured responses, the measured impulse responses exhibited faster oscillations in subsequent cycles than those predicted by the linear model. This is in line with the effects of nonlinear stiffness mentioned above. During the initial part of the impulse responses displacements are attained that are predominantly in the nonlinear range with reduced stiffness. The timing of the modeled impulse is synchronised to this phase (Fig. 5). When the oscillation envelope decays, a point is reached beyond which the gating compliance will hardly affect the cupular response, so that the effective stiffness during this phase is larger. The resonance frequency of an effectively stiffer cupula may accordingly be expected to increase when reaching these

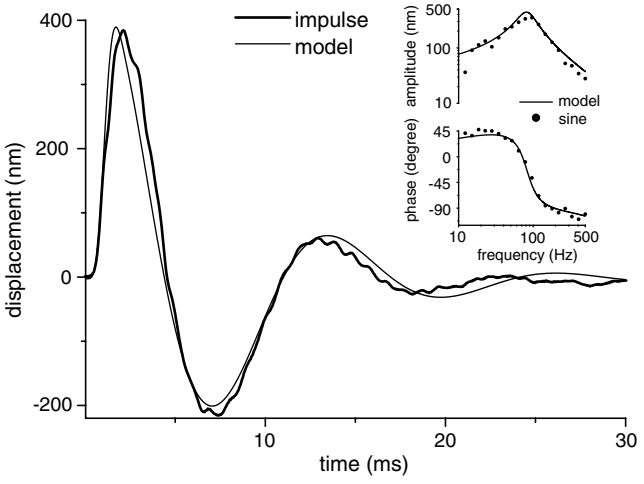

Fig. 5 Measured impulse response (*thick solid line*) compared with that calculated from the model (*thin solid line*), showing that the linear model cannot completely describe the timing of the crossings of the equilibrium position of the cupula. *Inset* Frequency response for the same cupula, with measured sinusoidal responses (*data points*) and fitted model (*solid lines*)

smaller (< 100 nm) oscillation amplitudes (van Netten 1997). This will result in smaller time lapses between successive equilibrium position crossings, as observed.

Significance of instantaneous onset of cupular responses and relaxation

The maximum deflection from equilibrium reached just after the onset of the stimulus impulse differs among cupulae. These variations, unlike the timing and resonance feartures, are not determined by cupular properties but primarily by variations of the imposed displacement amplitude of the local fluid flow, as produced by the stimulus sphere, at the location of the cupula. Such variations may easily arise from differences in the placement of the stimulus sphere relative to the cupula, which although being kept as constant as possible, varies slightly among experiments, also due to differences in canal shape and size. This independence from cupular properties can be appreciated from the frequency characteristics as depicted in Fig. 4a, which show that cupular displacement in response to high frequency (> 300 Hz) fluid displacement becomes frequency-independent. This indicates that the displacement of the cupula is equal to that of the excitatory fluid, which can be explained by inertial fluid forces dominating stiffness and viscous forces on the cupula in this high-frequency range.

Another important effect of this is that, in response to a fluid displacement step, the inertial fluid forces, which are associated with the high-frequency content of a step, cause a cupula to instantaneously respond to the fluid step displacement without delay and with the same displacement as the local fluid. This effect is clearly demonstrated in Fig. 2, which shows that the initial

displacement of the cupula follows the fluid displacement step produced by the stimulus sphere, within the accuracy of time measurement (< 0.1 ms). After this initial cupular displacement, viscous fluid forces damp the motion of the cupula. The transfer of surrounding water displacement into a lateral line canal is similarly controlled by inertial fluid forces at high frequencies (Denton and Gray 1983, 1989; S.M. van Netten (submitted)). Therefore, when a cupula is located in a canal, the initial water displacement step outside a fish is expected to be equally well transferred instantaneously, via the canal, into cupular motion.

Delay-less transient signals can obviously be of importance to an animal. In the natural habitat of a fish, fast signals might be essential for survival or prey detection, since a sudden displacement of the water might be produced by, for example, an attacking predator or prey. It has been suggested that such signals are mediated by the Mauthner system, on which lateral line afferents project (Eaton et al. 2002). Afferent lateral line activity in response to a transiently moving sphere was shown to occur within 5 ms after stimulus onset (Wubbels 1990).

Another important characteristic of the observed transient responses is the relaxation time, τ. This can be considered as a measure of the time that a cupula needs to recover to its equilibrium position after a displacement step. The relaxation time constant of the cupula of the ruffe was on average found to be less than 5 ms from fitting an exponential envelope to the damped oscillations that a cupula exhibits in response to a fluid velocity impulse. From considering the response properties of a damped mechanical oscillator, it follows that the relaxation time of a resonating cupula ($N_r >> 1$) is closely related to its quality factor: $\tau \cong Q/(\pi f_r)$ (van Netten). Use of the obtained quality factor ($Q_I = 1.8$) and resonance frequency ($f_{rI} = 121$ Hz) then yields a relaxation time constant, τ, of approximately 4.7 ms, in close agreement with the experimentally obtained mean result (4.4 ms).

From our present experiments, we may thus conclude that the hydrodynamics of the peripheral lateral line organ does not impose a limit on the time resolution of detection by the cupula of the onset of a step of water displacement.

Acknowledgements The authors thank D.G. Stavenga, G.R. Blake and A.B.A. Kroese for their comments on the manuscript. B.C-B. was supported by the School of Behavioural and Cognitive Neurosciences (BCN, University of Groningen). Animal procedures conformed to Dutch governmental rules and the guidelines of the University of Groningen Institutional Animal Care and Use Committee (*RuG-DEC*).

References

Abdel-Latif H, Hassan ES, von Campenhausen C (1990) Sensory performance of blind Mexican cave fish after destruction of the canal neuromasts. Naturwissenschaften 77:237–239

Bleckmann H (1993) Role of the lateral line in fish behaviour. In: Pitcher TJ (ed) Behaviour of Teleost fishes. Chapman and Hall, London, pp 201–246

Bleckmann H, Breithaupt T, Blickhan R, Tautz J (1991) The time course and frequency content of hydrodynamic events caused by moving fish, frogs, and crustaceans. J Comp Physiol A 168:749–757

Coombs S, Janssen J (1990) Behavioral and neurophysiological assessment of lateral line sensitivity in the mottled sculpin, Cottus bairdi. J Comp Physiol A 167:557–567

Denton EJ, Gray J (1983) Mechanical factors in the excitation of clupeid lateral lines. Proc R Soc Lond B Biol Sci 218:1–26

Denton EJ, Gray JA (1989) Some observations on the forces acting on neuromasts in fish lateral line canals. In: Coombs S, Görner P, Münz H (eds) The mechanosensory lateral line: neurobiology and evolution. Springer, Berlin Heidelberg New York, pp 229–246

Dijkgraaf S (1963) The functioning and significance of the lateral-line organs. Biol Rev 38:51–105

Eatock RA (2000) Adaptation in hair cells. Annu Rev Neurosci 23:285–314

Eaton RC, Casagrand JL, Cummins GI (2002) Neural implementation of the phase model for localising impulse sounds by the Mauthner system. Bioacoustics 12:209–212

Engelmann J, Hanke W, Mogdans J, Bleckmann H (2000) Hydrodynamic stimuli and the fish lateral line. Nature 408:51–52

Enger PS, Kalmijn AJ, Sand O (1989) Behavioral investigations of the function of the lateral line and inner ear in predation. In: Coombs S, Görner P, Münz H (eds) The mechanosensory lateral line: neurobiology and evolution. Springer, Berlin Heidelberg New York, pp 575–587

Hoekstra D, Janssen J (1985) Non-visual feeding behaviour of the mottled sculpin, *Cottus bairdi*, in Lake Michigan. Environ Biol Fishes 12:111–117

Hudspeth AJ, Choe Y, Mehta AD, Martin P (2000) Putting ion channels to work: mechanoelectrical transduction, adaptation, and amplification by hair cells. Proc Natl Acad Sci USA 97:11765–11772

Jakubowski J (1963) Cutaneou sense organs of fishes. I. The lateral-line organs in stone-perch (*Acerina cernua* L.). Acta Biol Cracov 6:59–78

Kalmijn AJ (1988) Hydrodynamic and acoustic field detection. In: Atema R, Fay RR, Popper AN, Tavolga WN (eds) Sensory biology of aquatic animals. Springer, Berlin Heidelberg New York, pp 83–130

Kalmijn AJ (1989) Functional evolution of lateral line and inner ear sensory systems. In: Coombs S, Görner P, Münz H (eds) The mechanosensory lateral line: neurobiology and evolution. Springer, Berlin Heidelberg New York, pp 187–215

Kroese ABA, Schellart NA (1992) Velocity- and acceleration-sensitive units in the trunk lateral line of the trout. J Neurophysiol 68:2212–2221

Kroese ABA, van Netten SM (1987) The application of incident light polarization microscopy for the visualization of vertebrate sensory hair cells in vivo. J Microsc 145:309–317

Kroese ABA, van Netten SM (1989) Sensory transduction in lateral line hair cells. In: Coombs S, Görner P, Münz H (eds) The mechanosensory lateral line. Springer, Berlin Heidelberg New York, pp 265–284

Kroese ABA, van der Zalm JM, van den Bercken J (1978) Frequency-response of the lateral-line Organ of *Xenopus-laevis*. Pflügers Archiv-Eur J Physiol 375:167–175

Montgomery JC, Macdonald JA (1987) Sensory tuning of lateral line receptors in antarctic fish to the movements of planktonic prey. Science 235:195–196

Montgomery JC, Baker CF, Carton AG (1997) The lateral line can mediate rheotaxis in fish. Nature 389:960–963

van Netten SM (1991) Hydrodynamics of the excitation of the cupula in the fish canal lateral line. J Acoust Soc Am 89:310–319

van Netten SM (1997) Hair cell mechano-transduction: its influence on the gross mechanical characteristics of a hair cell sense organ. Biophys Chem 68:43–52

van Netten SM, Khanna SM (1994) Stiffness changes of the cupula associated with the mechanics of hair cells in the fish lateral line. Proc Natl Acad Sci USA 91:1549–1553

van Netten SM, Kroese ABA (1987) Laser interferometric measurements on the dynamic behaviour of the cupula in the fish lateral line. Hear Res 29:55–61

Partridge BL, Pitcher TJ (1980) The sensory basis of fish schools: relative roles of lateral line and vision. J Comp Physiol 135:315–325

Russel IJ (1976) Amphibian lateral line receptors. In: Linas R, Precht W (eds) Frog neurobiology. Springer, Berlin Heidelberg New York, pp 513–550

Satou MHA, Takeuchi JN, Tanabe M, Kitamura S, Okumoto N, Iwata M (1994) Behavioral and electrophysiological evidence that the lateral line is involved in the inter-sexual vibrational communication of the hime salmon (landlocked red salmon, *Oncorhynchus nerka*). J Comp Physiol A 174:539–549

Stokes GG (1851) On the effect of the internal friction of fluids on the motion of pendulums. Trans Camb Philos Soc 9:6–106

Tsang PTSK (1997) Laser interferometric flow measurements in the lateral line organ. Thesis, University of Groningen, Groningen

Tsang PTSK, van Netten SM (1997) Fluid flow profiles measured in the supraorbital lateral line canal of the ruff. In: Lewis ER, Long GR, Lyon RF, Narins PM, Steele CR, Hecht-Poinar E (eds) Diversity in auditory mechanics. World Scientific, Singapore, pp 25–31

Wiersinga-Post JEC, van Netten SM (2000) Temperature dependency of cupular mechanics and hair cell frequency selectivity in the fish canal lateral line organ. J Comp Physiol A 186:949–956

Wubbels RJ (1990) Afferent activity in the supra-orbital canal of the ruff lateral line. Thesis, University of Groningen, Groningen

Wubbels RJ (1992) Afferent response of a head canal neuromast of the Ruff (*Acerina-cernua*) lateral line. Comp Biochem Physiol 102:19–26